Title: Quantitative Assessment of Column-Specific Degeneration in Cervical Spondylotic Myelopathy based on Diffusion Tensor Tractography

Running Title: Tractography-based quantification in CSM

Jiao-Long Cui, Xiang Li, Tin-Yan Chan, Kin-Cheung Mak, Keith Dip-Kei Luk, Yong Hu*****

Department of Orthopaedics and Traumatology, the University of Hong Kong

"*****" Correspondence Author

Dr. Yong Hu

Dept. of Orthopeadics and Traumatology,

The University of Hong Kong

Address: 12 Sandy Bay Road, Pokfulam, Hong Kong

Email address: yhud@hku.hk;

Tel: (852) 29740359; Fax: (852) 29740335

Acknowledgements

The authors would like to thank the support from the General Research Fund from The University Grant Council of Hong Kong (771608M/774211M). The authors would like to thank Dr. Henry Mak for his assistant in MRI scanning.

Abstract

PURPOSE Cervical spondylotic myelopathy (CSM) is a common spinal cord disorder in the elderly. Diffusion tensor imaging (DTI) has been shown to be of great value for evaluating the microstructure of nerve tracts in the spinal cord. Currently, the quantitative assessment of the degeneration on the specific tracts in CSM is still rare. The aim of the present study was to use tractography-based quantification to investigate the column-specific degeneration in CSM.

METHODS A total of 43 volunteers were recruited with written informed consent, including 20 healthy subjects and 23 CSM patients. Diffusion MRI was taken by 3T MRI scanner. Fiber tractography was performed using TrackVis to reconstruct the white matter tracts of the anterior, lateral and posterior column on the bilateral sides. The DTI metrics acquired from tractography, including fractional anisotropy (FA), mean diffusivity (MD), axial diffusivity (AD) and radial diffusivity (RD), were compared between healthy subjects and CSM patients.

RESULTS Compared to healthy subjects, FA was found significantly lower in the lateral (Healthy 0.64 ± 0.07 vs. CSM 0.53 ± 0.08) and posterior column (Healthy 0.67 ± 0.08 vs. CSM 0.47 ± 0.08) ($p<0.001$), while MD, AD and RD were significantly higher in the anterior, lateral and posterior column in CSM ($p<0.05$).

CONCLUSION Loss of microstructural integrity was detected in the lateral and posterior column in CSM. Tractography-based quantification was capable of evaluating the subtle pathological insult within white matter on a column-specific basis, which exhibited potential clinical value for in vivo evaluation of the severity of CSM

Key words: Diffusion tensor imaging, Tractography, Cervical spondylotic myelopathy, Spinal cord, Fractional anisotropy

Introduction

Cervical spondylotic myelopathy (CSM) is a common type of spinal disorder associated with chronic spinal cord compression in a canal narrowed by degenerative disc and spondylosis [1, 2]. The symptoms and signs of CSM vary, such as abnormal gait, weakness or stiffness of legs, numb and clumsy hands, neck stiffness, stabbing pain in the arms [3]. Damage to specific white matter tracts within the spinal cord can often result in the particular neurological deficits and symptoms. However, the neurological examination may vary among different clinicians and is difficult to quantify the neurological deficit objectively. Therefore, to quantify the pathological impairment in each column of white matter exhibits great clinical value in supplementing the shortage of neurological evaluation. Moreover, a better understanding of column-specific white matter damage could enable us to further reveal the underlying pathomechanism of CSM.

Diffusion tensor imaging (DTI) is an in vivo imaging tool for evaluating the microstructural changes in the chronic compressive spinal cord [4]. Derived from the diffusion matrix, three eigenvalues and three eigenvectors represent the strength and orientation of the diffusion respectively. DTI metrics fractional anisotropy (FA), mean diffusivity (MD), axial diffusivity (AD) and radial diffusivity (RD) are generated from eigenvalues to quantify the microstructural integrity [5]. In the previous studies, due to the limited signal-to-noise ratio (SNR) and cross-sectional resolution of spinal cord DTI, the dominant approach for quantifying DTI metrics in CSM was to manually draw regions of interest (ROIs) on the sagittal section or the whole cord of axial section [6-12]. ROIs included both gray and white matter, which led to the loss of regional details. In addition, hand-drawn ROI method is highly time-consuming and user-dependent [4]. Especially in CSM, The deformation and degeneration of the cord makes difficulties for users to define ROIs and may result in operator bias. Till now, the quantification of DTI metrics on the specific tracts in CSM was still

lacking.

Recently, there are growing interests in tractography-based quantification of DTI metrics in the spinal cord. Tractography-based quantification consists of first reconstructing the underlying fiber bundles via tractography algorithms. Once the tracts are reconstructed, the DTI metrics within the tracts can be quantified [4, 13]. Tractography-based quantification outperforms hand-drawn ROI in terms of the following two aspects: 1) it is possible to pre-define seed points in various regions of the spinal cord for selective tract generation, and so quantify metrics in specific nerve tracts; 2) it is a semi-automatic procedure and it has relatively low operator bias. In the present study, we aim to employ diffusion tensor tractography to detect the column-specific degeneration in CSM.

Materials and Methods

Subjects

The institutional review board of research ethics approved all experimental procedures in this study. All volunteers were screened to confirm their eligibility. The inclusion criteria for healthy subjects were those having intact sensory and motor function evaluated, and negative Hoffman's sign under physical examination. Subjects having any neurological signs and symptoms or any past history of neurological injury, disease, or operations were excluded. CSM patients were recruited in author's institute. Experienced spine surgeons made a clinical diagnosis of CSM based on the patients' symptoms and signs as well as radiological findings. The neurological function of CSM patients were systemically evaluated using Japanese Orthopedic Association (JOA) scoring system [14], which indicates the overall functional assessment covering motor, sensory and sphincter functions. Ten second test was conducted as myelopathic hand signs to evaluate the degree of dysfunction of hand in CSM [15].

MRI Scanning

All images were taken via 3T MRI scanner (Philips Achieva, the Netherland). During the acquisition process, the subject was placed supine with head & neck coil enclosing the cervical region. The subject was then scanned with the anatomical T1-weighted (T1W), T2-weighted (T2W) images and DTI.

Sagittal and axial T1W and T2W images were acquired for each subject using fast spin echo sequence. For sagittal imaging, the imaging parameters were as follows: Field of view (FOV) = 250×250 mm, voxel size= 0.49×0.49 mm^2 in-plane, slice thickness = 3 mm, slice gap = 0.3 mm, fold-over direction = Feet/Head (FH), Number of excitation (NEX) = 2, Time of echo (TE) / Time of Repetition (TR) = 7.2 / 530 ms (T1W) and 120 / 3314 ms (T2W). A total of 11 sagittal images covering the whole cervical spinal cord were acquired. For axial imaging, a total of 12 transverse images covering the cervical spinal cord from C1 to C7 were acquired. The imaging parameters were as follows: FOV = 80×80 mm, voxel size= 0.56×0.56 mm^2 (T1W) and 0.63×0.63mm^2 (T2W) in-plane, slice thickness = 7 mm, fold-over direction = anterior/posterior (AP), NEX = 3, TE / TR = 8 / 1000 ms (T1W) and 120 / 4000 ms (T2W).

Diffusion MRI images were acquired using the sequence: single-shot spin-echo echo-planar imaging (SE-EPI). Diffusion encoding was in 15 non-collinear and non-coplanar diffusion directions with b-value = 600 s/mm^2. Spectral presaturation with inversion recovery was applied to avoid water-fat-shift artifacts. Cardiac vectorcardiogram triggering was applied to minimize the pulsation artifact from cerebrospinal fluid [16]. The imaging parameters were as follows: FOV = 80×36 mm, acquisition matrix= 80×28, reconstructed resolution = 0.63×0.63, slice thickness = 7 mm, fold-over direction = AP, NEX= 3, EPI factor=35, TE / TR = 60 ms / 5 heartbeats. The image slice planning was the same as the anatomical axial T2W images, with 12 slices covering the cervical spinal cord from C1 to C7. The mean duration of DTI was

24 minutes per subject with an average heart rate of 60 beats per minute.

Post-processing of Diffusion Tensor Fiber Tractography

Tensor reconstruction and fiber tractography were employed via Diffusion Toolkit v0.5. The maps of FA, three eigenvalues (λ1, λ2 and λ3) and corresponding eigenvectors were acquired. Tract visualization and DTI metrics quantification were performed using TrackVis v0.6 (**www.trackvis.org**, Harvard Medical School, Boston, USA). Fiber assignment by continuous tracking (FACT) was performed as propagation algorithm and diffusion weighted imaging (DWI) mask was automatically applied to filter the tracking [17, 18]. The maximum turning angle threshold was set as 35 degrees, in line with the previous studies [19]. Seeding masks was manually drawn by expert radiologists on FA map at the level of C2 (Fig. 1) in line with the previous study, including the whole cord and anterior, lateral and posterior column of white matter on the bilateral sides. The mean value of FA, MD, AD, and RD was acquired. After the measurement of track to voxel count via TrackVis, the density of tracked fibers was calculated as the ratio of the track to voxel count [13].

Statistical Analysis

The comparisons of fiber density, FA, MD, AD and RD were performed between healthy subjects and CSM patients using two-tailed unpaired Student's t-test. All values were reported as mean±SD and MD, AD and RD value were in 1×10^{-3} mm^2/s. The level of significance was set at $p<0.05$. The statistical analyses were performed using SPSS 15.0 software (SPSS Inc, Chicago, IL, USA).

Results

A total of 43 volunteers, including 20 adult healthy subjects (46±11 years old) and 23 CSM patients (59±12 years old), met with the inclusive criteria were enrolled in this study. CSM

patients showed lower JOA scores (CSM: 11±3 vs. full score: 17). The clinical details of included CSM patients were exhibited in Table 1. Diffusion MR images were successfully acquired in all healthy subjects and CSM patients. As shown in Fig. 2, butterfly-shaped gray matter was clearly seen in the FA image of healthy cord. In the contrary, it was very difficult to differentiate the gray matter from white matter in the degenerative cord.

Fiber tractography has been successfully performed in all volunteers to quantify the DTI metrics. As shown in Fig. 3, the fiber density in the whole cord and anterior column of healthy subjects was significantly higher than that in CSM (whole cord: Healthy 0.32±0.03 vs. CSM 0.29±0.04, $p<0.05$; anterior column: Healthy 0.34±0.04 vs. CSM 0.28±0.06, $p<0.001$), but no significant difference in fiber density was observed between healthy and myelopathic cord in the lateral (Healthy 0.36±0.07 vs. CSM 0.34±0.07, $p>0.05$) and posterior column (Healthy 0.37±0.05 vs. CSM 0.37±0.06, $p>0.05$).

The FA value significantly decreased in CSM in comparison to healthy subjects in the whole cord (Healthy 0.62±0.07 vs. CSM 0.54±0.08, $p<0.01$), lateral column (Healthy 0.64±0.07 vs. CSM 0.53±0.08, $p<0.001$) and posterior column (Healthy 0.67±0.07 vs. CSM 0.47±0.08, $p<0.001$). There was no significant difference in the anterior column between healthy subjects (0.58±0.10) and CSM (0.57±0.07, $p>0.05$). It was indicated that CSM exhibited significant higher MD (whole cord: Healthy 1.15±0.30 vs. CSM 1.49±0.37, $p<0.001$; anterior column: Healthy 1.22±0.31 vs. CSM 1.47±0.37, $p<0.001$; lateral column: Healthy 1.16±0.28 vs. CSM 1.53±0.36, $p<0.001$; posterior column: Healthy 1.06±0.31 vs. CSM 1.49±0.37, $p<0.001$), AD (whole cord: Healthy 2.11±0.33 vs. CSM 2.53±0.48, $p<0.01$; anterior column: Healthy 2.14±0.39 vs. CSM 2.54±0.49, $p<0.001$; lateral column: Healthy 2.14±0.38 vs. CSM 2.62±0.48, $p<0.001$; posterior column: Healthy 2.10±0.35 vs. CSM 2.63±0.51, $p<0.001$) and RD value (whole cord: Healthy 0.67±0.31 vs. CSM 0.96±0.33,

p<0.01; anterior column: Healthy 0.77±0.33 vs. CSM 0.94±0.34, p<0.05; lateral column: Healthy 0.67±0.31 vs. CSM 0.98±0.33, p<0.001; posterior column: Healthy 0.55±0.32 vs. CSM 0.92±0.34, p<0.001) than healthy subjects .

Discussion

This study employed diffusion tensor tractography to measure column-specific diffusion property in CSM. Under the chronic compression, the degree of microarchitectural integrity in CSM significantly decreased in the lateral and posterior column of white matter in comparison to healthy subjects, while there was no significant difference in the anterior column. It was the first investigation, to our best knowledge, of the degeneration of specific tracts in CSM via tractography-based DTI metrics quantification.

FA is the most commonly used DTI parameters to indicate the microstructural integrity [19]. It reflects the degree of diffusion anisotropic in one particular voxel, mainly indicating structural characteristics of white matter (e.g., axonal diameter, fiber density, and myelination) [20]. As shown in the present study, the change of the FA and MD value in the whole spinal cord in CSM compared to healthy subjects were consistent with the previous findings [8, 21], i.e. decrease in FA and increase in MD. In case that the cord compression mainly locates unilaterally, the degeneration of white matter tracts may distribute disproportionately between two sides of the cord. The DTI metrics changes of localized degeneration within one or several tracts on the compromised side may not be sensitive enough to distinguish the existence and magnitude of abnormality with the whole cord analysis. Thereby, upon the most previous CSM studies that the FA value was only obtained in the whole cord, the FA value in each white matter tract was also measured in current study, which could particularly quantify the tract-specific degeneration. For instance, as shown in Fig. 4, it was the sagittal T2W and axial FA image of case 15, who was a 46-year-old male and presented numbness and

clumsiness of left hand as well as spasticity of left lower limb. The overall neurologic dysfunction was evaluated with the JOA score (11.5/17) and 10 second test showed significant deterioration in left hand rather than the right (4 versus 24). The axial image showed the cord compression at level C45 was mainly on the left side. With DTI analysis, we found the FA value of the whole cord is 0.57. Compared to the mean FA value of healthy cord 0.62 ± 0.07, the FA value of whole cord on the compression level of this case was not significantly lower. The FA value measured in the anterior, lateral and posterior column of white matter was 0.51, 0.48, 0.46 on the left side and 0.62, 0.63, 0.65 on the right side respectively. It revealed that the FA value on the left side was much lower than that on the right side. The low FA value of the lateral and posterior column on the left side corresponded with the clumsiness and numbness of the limbs on the same side. It indicated that DTI was capable of providing the quantitative evaluation of the subtle pathological insult within white matter on a column-specific basis, complementary to neurological diagnosis.

The degeneration of the sensory tracts in the posterior columns revealed by DTI may explain the clinical manifestation in the majority of CSM patients, i.e. sensory disturbance of four limbs and gait disturbance. The degeneration of corticospinal tract in the lateral column of white matter may account for intrinsic hand muscle wasting and disability of hands and fingers. In our result, the significant decreased value of FA, which suggested the loss of microstructural integrity after chronic compression, was notable in the posterior and lateral column. This result is corresponding with the deficit of JOA score and 10 second test in this cohort of patients. Furthermore, the decrease of FA in the anterior column of white matter was not significant. The finding was also in line with the limited clinical autopsy data showing that the lateral corticospinal tracts and posterior column were commonly affected by the anterior compression with relatively sparing anterior column [22, 23].

There were several limitations in this study. First, CSM is a result of age-related degeneration of the cervical spine. However, for the small number of the subjects recruited in this study, the age of healthy subjects (approximately 46 years) was younger than that in the patient group (approximately 59 years). This potentially confounding factor should be controlled in a future large-scale population study. Second, the 7mm thickness of axial slice resulted in a higher degree of isotropic of image voxel comparing with the previous studies (3 or 5mm thickness). It should also be noted that there was only a single orientation for one voxel in fiber tractography. As a result, the highly isotropic voxel may lead to the loss of orientational information along the cord. Third, partial volume effect may also exist under the 0.63×0.63 mm^2 in-plane resolution, which resulted in the positive false for tractography. Therefore, the tracked fiber bundles were double checked by the expert radiologists and orthopedic surgeons. In addition, this study focused on the fiber tracts along the cord but missed the segmental measurements. In future, application of this column-specific measurement for the level diagnosis in CSM was highly appreciated.

In summary, tractography-based DTI measurements could quantify the degeneration of the specific tracts in CSM. Loss of microstructural integrity was detected in the lateral and posterior column of white matter. The quantification of column-specific degeneration based on fiber tractography might be a precision tool for in-vivo evaluation of the severity of CSM and monitoring the disease progression.

Acknowledgements

The authors would like to thank the support from the General Research Fund from The University Grant Council of Hong Kong (771608M/774211M). The authors would like to thank Dr. Henry Mak for his assistant in MRI scanning.

References

1. Ichihara K, Taguchi T, Sakuramoto I, Kawano S, Kawai S (2003) Mechanism of the spinal cord injury and the cervical spondylotic myelopathy: new approach based on the mechanical features of the spinal cord white and gray matter. Journal of neurosurgery 99:278-285

2. Rao R (2003) Neck pain, cervical radiculopathy, and cervical myelopathy: pathophysiology, natural history, and clinical evaluation. Instructional course lectures 52:479-488

3. Baron EM, Young WF (2007) Cervical spondylotic myelopathy: a brief review of its pathophysiology, clinical course, and diagnosis. Neurosurgery 60:S35-41. doi: 10.1227/01.NEU.0000215383.64386.82

4. Stroman PW, Wheeler-Kingshott C, Bacon M, Schwab JM, Bosma R, Brooks J, Cadotte D, Carlstedt T, Ciccarelli O, Cohen-Adad J, Curt A, Evangelou N, Fehlings MG, Filippi M, Kelley BJ, Kollias S, Mackay A, Porro CA, Smith S, Strittmatter SM, Summers P, Tracey I (2014) The current state-of-the-art of spinal cord imaging: Methods. NeuroImage 84:1070-1081. doi: 10.1016/j.neuroimage.2013.04.124

5. Mukherjee P, Berman JI, Chung SW, Hess CP, Henry RG (2008) Diffusion tensor MR imaging and fiber tractography: theoretic underpinnings. AJNR American journal of neuroradiology 29:632-641. doi: 10.3174/ajnr.A1051

6. Song T, Chen WJ, Yang B, Zhao HP, Huang JW, Cai MJ, Dong TF, Li TS (2011) Diffusion tensor imaging in the cervical spinal cord. European spine journal : official publication of the European Spine Society, the European Spinal Deformity Society, and the European Section of the Cervical Spine Research Society 20:422-428. doi: 10.1007/s00586-010-1587-3

7. Cui JL, Wen CY, Hu Y, Li TH, Luk KD (2011) Entropy-based analysis for diffusion anisotropy mapping of healthy and myelopathic spinal cord. NeuroImage 54:2125-2131. doi: 10.1016/j.neuroimage.2010.10.018

8. Xiangshui M, Xiangjun C, Xiaoming Z, Qingshi Z, Yi C, Chuanqiang Q, Xiangxing M, Chuanfu L, Jinwen H (2010) 3 T magnetic resonance diffusion tensor imaging and fibre tracking in cervical myelopathy. Clinical radiology 65:465-473. doi: 10.1016/j.crad.2010.01.019

9. Uda T, Takami T, Tsuyuguchi N, Sakamoto S, Yamagata T, Ikeda H, Nagata T, Ohata K (2013) Assessment of cervical spondylotic myelopathy using diffusion tensor magnetic resonance imaging parameter at 3.0 tesla. Spine 38:407-414. doi: 10.1097/BRS.0b013e31826f25a3

10. Wen CY, Cui JL, Liu HS, Mak KC, Cheung WY, Luk KD, Hu Y (2013) Is Diffusion Anisotropy a Biomarker for Disease Severity and Surgical Prognosis of Cervical Spondylotic Myelopathy? Radiology. doi: 10.1148/radiol.13121885

11. Jones JG, Cen SY, Lebel RM, Hsieh PC, Law M (2013) Diffusion tensor imaging correlates with the clinical assessment of disease severity in cervical spondylotic myelopathy and predicts outcome following surgery. AJNR American journal of neuroradiology

34:471-478. doi: 10.3174/ajnr.A3199

12. Cui JL, Wen CY, Hu Y, Mak KC, Mak KH, Luk KD (2011) Orientation entropy analysis of diffusion tensor in healthy and myelopathic spinal cord. NeuroImage 58:1028-1033. doi: 10.1016/j.neuroimage.2011.06.072

13. Wen CY, Cui JL, Lee MP, Mak KC, Luk KD, Hu Y (2013) Quantitative analysis of fiber tractography in cervical spondylotic myelopathy. The spine journal : official journal of the North American Spine Society 13:697-705. doi: 10.1016/j.spinee.2013.02.061

14. Yonenobu K, Abumi K, Nagata K, Taketomi E, Ueyama K (2001) Interobserver and intraobserver reliability of the japanese orthopaedic association scoring system for evaluation of cervical compression myelopathy. Spine 26:1890-1894; discussion 1895

15. Ono K, Ebara S, Fuji T, Yonenobu K, Fujiwara K, Yamashita K (1987) Myelopathy hand. New clinical signs of cervical cord damage. The Journal of bone and joint surgery British volume 69:215-219

16. Summers P, Staempfli P, Jaermann T, Kwiecinski S, Kollias S (2006) A preliminary study of the effects of trigger timing on diffusion tensor imaging of the human spinal cord. AJNR American journal of neuroradiology 27:1952-1961

17. Gasparotti R, Lodoli G, Meoded A, Carletti F, Garozzo D, Ferraresi S (2013) Feasibility of diffusion tensor tractography of brachial plexus injuries at 1.5 T. Investigative radiology 48:104-112. doi: 10.1097/RLI.0b013e3182775267

18. Moldrich RX, Pannek K, Hoch R, Rubenstein JL, Kurniawan ND, Richards LJ (2010) Comparative mouse brain tractography of diffusion magnetic resonance imaging. NeuroImage 51:1027-1036. doi: 10.1016/j.neuroimage.2010.03.035

19. Thurnher MM, Law M (2009) Diffusion-weighted imaging, diffusion-tensor imaging, and fiber tractography of the spinal cord. Magnetic resonance imaging clinics of North America 17:225-244. doi: 10.1016/j.mric.2009.02.004

20. Lindberg PG, Feydy A, Maier MA (2010) White matter organization in cervical spinal cord relates differently to age and control of grip force in healthy subjects. The Journal of neuroscience : the official journal of the Society for Neuroscience 30:4102-4109. doi: 10.1523/JNEUROSCI.5529-09.2010

21. Lee JW, Kim JH, Park JB, Park KW, Yeom JS, Lee GY, Kang HS (2011) Diffusion tensor imaging and fiber tractography in cervical compressive myelopathy: preliminary results. Skeletal radiology 40:1543-1551. doi: 10.1007/s00256-011-1161-z

22. Ogino H, Tada K, Okada K, Yonenobu K, Yamamoto T, Ono K, Namiki H (1983) Canal diameter, anteroposterior compression ratio, and spondylotic myelopathy of the cervical spine. Spine 8:1-15

23. Fehlings MG, Skaf G (1998) A review of the pathophysiology of cervical spondylotic myelopathy with insights for potential novel mechanisms drawn from traumatic spinal cord injury. Spine 23:2730-2737

Figures Legends

Fig. 1 The representative image demonstrated the column-specific tractography. The whole cord tractography was performed by seeding at C2 level (A). The red arrow indicated the compressive site. The ROIs were drawn on the normal-appearing cord of C2 level to select the anterior, lateral and posterior column of white matter (B). The fiber bundles of each column were selected (C). The enlarged image showed that the fiber bundles passed through the compressive cord (D). The projection of the tracts on the axial map indicated the location of each column in the cross-section (E). A: anterior; P: posterior; L: left; R: right

Fig. 2 The representative images showed the C34 level of the healthy cord (upper row) and the myelopathic cord (lower row) in the sagittal T2W image (A, D), axial T2W image (B, E) and axial FA image (C, F). In the healthy cord, the butterfly-shaped gray matter could be clearly observed in FA image (C). The gray matter was difficult to be differentiated in the degenerative cord under compression (F). A: anterior; P: posterior; R: right; L: left

Fig. 3 Comparison of DTI metrics between the healthy and myelopathic spinal cord (Mean ± SD). FD: fiber density (tract/voxel), MD, AD and RD value are in 1×10^{-3} mm^2/s. (Significant differences are indicated by *$p<0.05$, ** $p<0.01$ and *** $p<0.001$)

Fig. 4 A 46-year-old male (patient number 15) with JOA score of 11.5. Sagittal T2W imaging demonstrated the compression at the intervertebral level C45 (A). The axial FA image at level C45 showed that the compression was mainly on the left side (B). A: anterior; P: posterior; R: right; L: left

Figure 1
Click here to download high resolution image

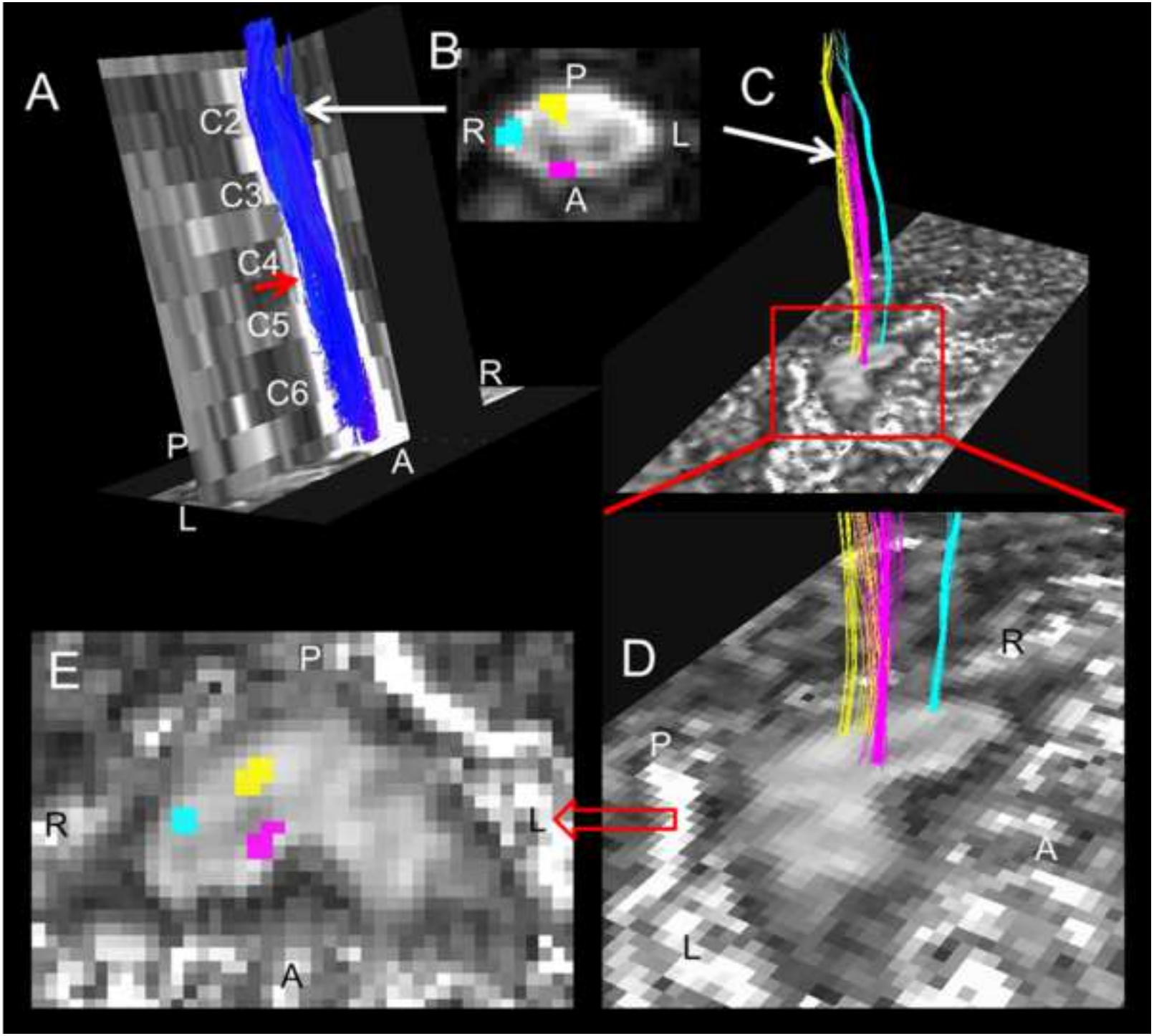

Figure 2
Click here to download high resolution image

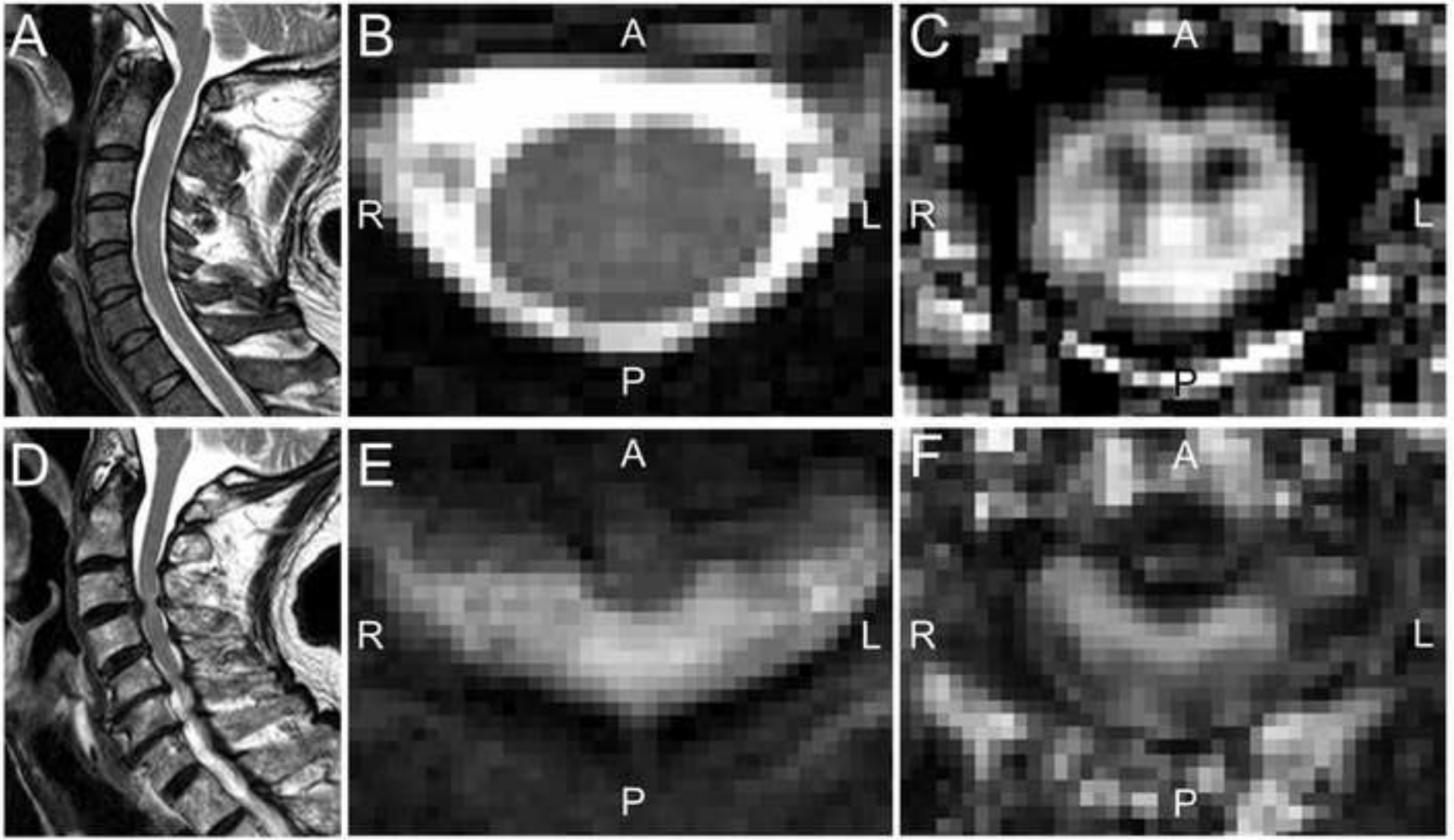

Figure 3
Click here to download high resolution image

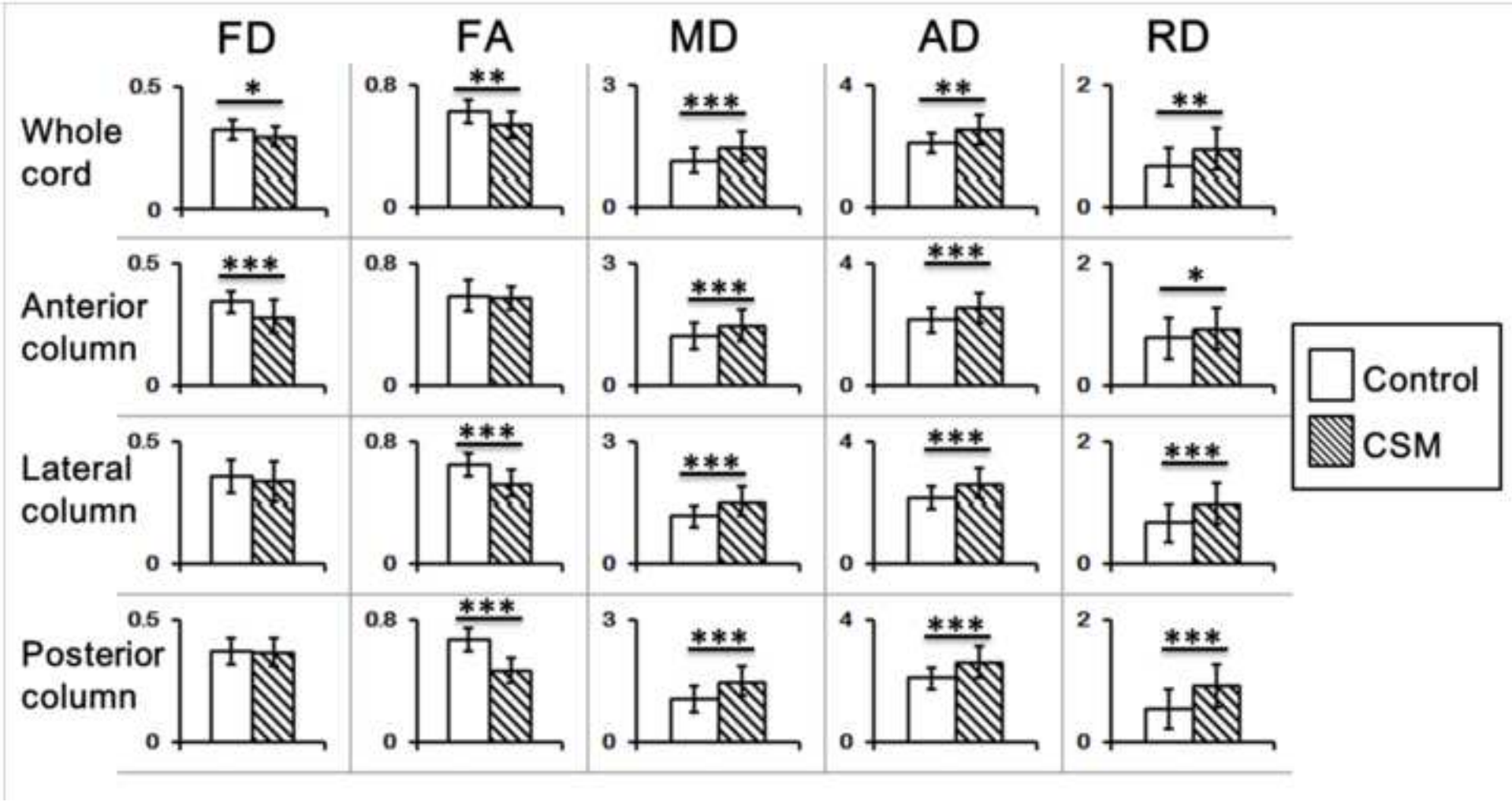

Figure 4
Click here to download high resolution image

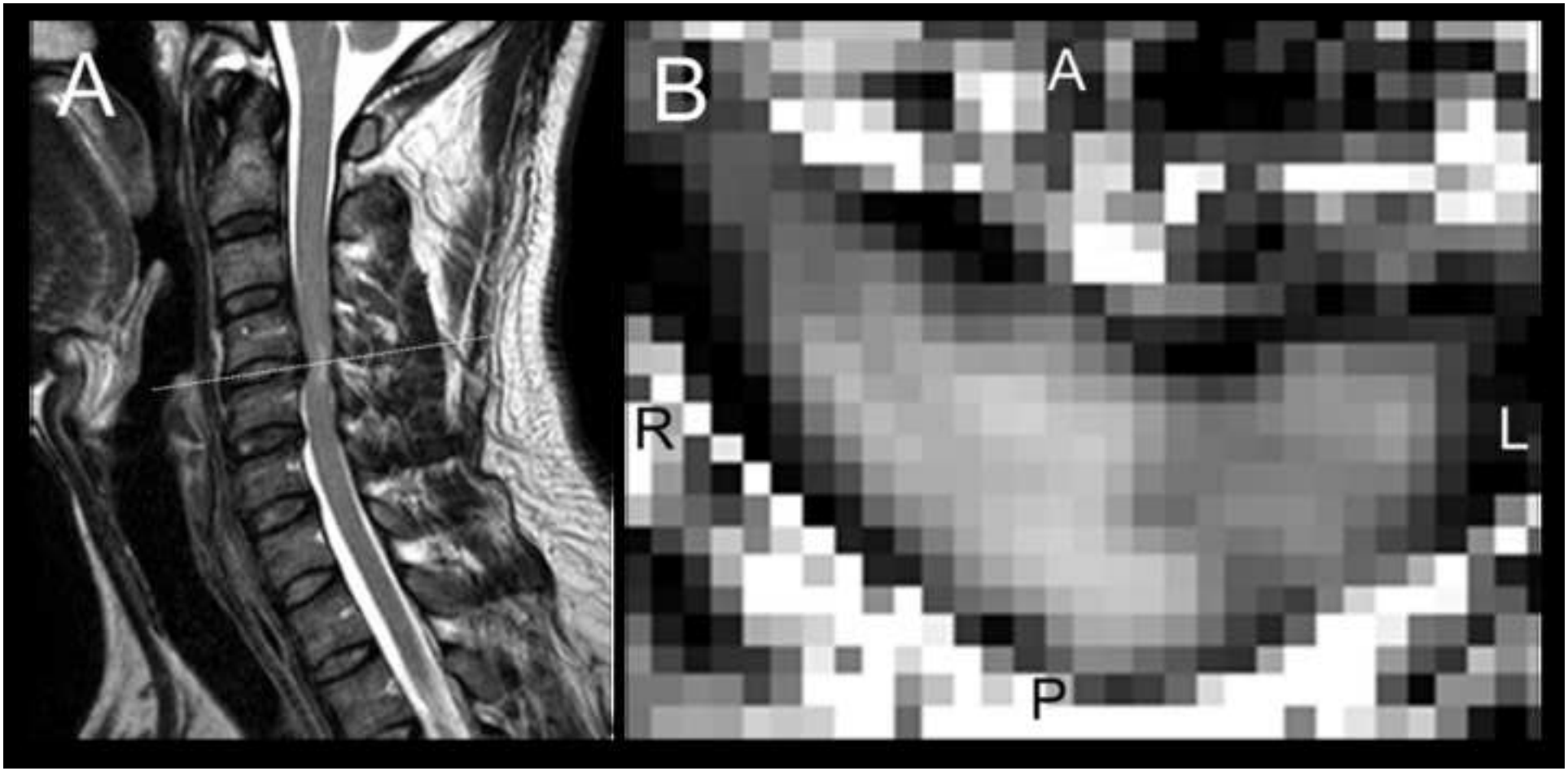

Table 1

Table 1 Clinical details of included patients

Case no.	Gender	Age(years)	JOA	10sec(L)	10sec(R)	Symptom	Sympton Duration	Level of compression
1	M	73	7.5	5	6	Gait disturbance	1y	C45, C56
2	M	76	7.5	22	15	Clumsiness in both hands	2m	C34, C45, C56
3	F	52	7	13	14	Numbness and clumsiness in both hands	5m	C34, C45, C56
4	F	44	11.5	12	8	Numbness of the hands and lower limbs	2y	C45, C56
5	M	46	11	20	20	Clumsiness in both hands	2y	C45
6	F	47	11	24	24	Numbness of bilat hands and lower limbs	4-5y	C56,C67
7	M	67	13	18	23	Gait disturbance	10y	C45, C56
8	F	68	14.5	15	20	Numbness and clumsiness in both hands	1m	C45, C56
9	F	71	17	22	24	Weakness in left upper limb	10y	C45
10	M	57	12.5	11	12	Numbness in both hands	1y	C34, C45, C56
11	M	54	4	19	6	Gait disturbance	4m	C34, C45
12	M	62	13.5	23	23	Left hands numbness and gait disturbance	7m	C56,C67,C71
13	M	45	7.5	8	8	Hands numbness and gait disturbance	4m	C34, C45
14	M	56	13	26	27	Numbness in both hands	6m	C34, C56
15	M	46	11.5	4	24	Left hand clumsiness	7m	C45, C56
16	M	55	13	23	22	Hands numbness and gait disturbance	2y	C45, C56
17	M	75	3.5	10	13	Neck pain and numbness in both arms and legs	5m	C45
18	M	76	10.5	18	18	Bilateral upper limb clumsiness and unsteadiness of gait	1y	C45, C56
19	M	49	15	16	16	Neck pain and persistent bilateral lower limb weakness and clumsiness	7y	C34, C45
20	F	84	10.5	20	20	Bilateral hands and toes numbness	12y	C34, C45, C56
21	F	53	15	20	20	Bilateral hands numbness and weakness	10m	C45
22	F	51	11.5	11	14	Unsteady gait, bilateral hand clumsiness and numbness	9m	C34, C45
23	M	58	9	20	28	Bilateral leg and trunk numbness, difficulty in balancing	1y	C34, C45, C56